International Journal of Cardiology 274 (2019) 144–151

Contents lists available at ScienceDirect

International Journal of Cardiology

journal homepage: www.elsevier.com/locate/ijcard

Electro-mechanical (dys-)function in long QT syndrome type 1☆

David Ziupa [a,b], Marius Menza [b,c], Susanne Koppermann [a,b], Robin Moss [b,d], Julia Beck [a,b], Gerlind Franke [a,b], Stefanie Perez Feliz [a,b], Michael Brunner [b], Sonja Mayer [a,b], Heiko Bugger [a,b], Gideon Koren [e], Manfred Zehender [a,b], Bernd A. Jung [b,c], Gunnar Seemann [b,d], Daniela Foell [a,b], Christoph Bode [a,b], Katja E. Odening [a,b,*]

[a] Department of Cardiology and Angiology I, Heart Center, University of Freiburg, Freiburg, Germany
[b] Faculty of Medicine, University of Freiburg, Freiburg, Germany
[c] Department of Radiology, Medical Physics, University Medical Center Freiburg, Freiburg, Germany
[d] Institute of Experimental Cardiovascular Medicine, Heart Center, University of Freiburg, Freiburg, Germany
[e] Cardiovascular Research Center, Division of Cardiology, Rhode Island Hospital, Alpert Medical School of Brown University, Providence, RI, USA

ARTICLE INFO

Article history:
Received 13 March 2018
Received in revised form 18 May 2018
Accepted 6 July 2018
Available online 9 July 2018

Keywords:
Long QT syndrome
Electro-mechanical dysfunction
Tissue-phase mapping cardiac MRI
I_{Kr}-blockade
Genotype differences

ABSTRACT

Background: Prolonged repolarization is the hallmark of long QT syndrome (LQTS), which is associated with subclinical mechanical dysfunction. We aimed at elucidating mechanical cardiac function in LQTS type 1 (loss of I_{Ks}) and its modification upon further prolongation of the action potential (AP) by I_{Kr}-blockade (E-4031).
Methods: Transgenic LQT1 and wild type (WT) rabbits ($n = 12/10$) were subjected to tissue phase mapping MRI, ECG, and epicardial AP recording. Protein and mRNA levels of ion channels and Ca^{2+} handling proteins ($n = 4/4$) were determined. *In silico* single cell AP and tension modeling was performed.
Results: At baseline, QT intervals were longer in LQT1 compared to WT rabbits, but baseline systolic and diastolic myocardial peak velocities were similar in LQT1 and WT. E-4031 prolonged QT more pronouncedly in LQT1. Additionally, E-4031 increased systolic and decreased diastolic peak velocities more markedly in LQT1 – unmasking systolic and diastolic LQT1-specific mechanical alterations. E-4031-induced alterations of diastolic peak velocities correlated with the extent of QT prolongation.
Conclusion: While baseline mechanical function is normal in LQT1 despite a distinct QT prolongation, further prolongation of repolarization by I_{Kr}-blocker E-4031 unmasks mechanical differences between LQT1 and WT with enhanced systolic and impaired diastolic function only in LQT1. These data indicate an importance of the *extent* of QT prolongation and the contribution of different impaired ion currents for conveying mechanical dysfunction.

1. Introduction

Dysfunction of repolarizing ion channels constitutes the pathophysiological link between inherited [1] and acquired [2] long QT syndromes (LQTS), which are both characterized by prolonged cardiac repolarization and an increased risk for ventricular tachycardia (VT) and sudden cardiac death. Inherited long QT syndromes type 1 (LQT1, loss-of-function mutations in *KCNQ1*/KvLQT1, reduction of I_{Ks}) and type 2 (LQT2, loss-of-function mutations in *KCNH2*/HERG, reduction of I_{Kr}) represent >80% of LQTS subtypes [1].

In addition to electrical dysfunction (*i.e.*, prolonged repolarization) [3], (subclinical) mechanical dysfunction is present in LQTS: In 1991, Nador et al. described for the first time left ventricular wall motion abnormalities in patients with LQTS, consisting of a more rapid early contraction and slowed/prolonged late contraction [4]. These abnormalities were present in 55% of LQTS patients (but only 5% of controls), and more frequent in symptomatic than asymptomatic LQTS patients (77% *vs.* 19%) [4]. After this initial important observation, several studies confirmed that LQTS is not a "purely electrical" disease, but does affect cardiac mechanical function with prolonged contraction duration and increased dispersion of contraction duration [5–12]. Prolonged contraction duration was demonstrated in LQTS patients by strain echocardiography [6–8] and tissue phase mapping MRI (TPM-MRI) [9]. Genotype differences in its extent have been postulated as the extent of the reduction of longitudinal strain was less pronounced in LQT1 [8]. These alterations in systolic or diastolic function in LQTS do not result in clinical overt heart failure, but its extent seems to correlate with the arrhythmic risk [6–9].

We previously generated transgenic rabbit models of LQT1 (KvLQT1-Y315S, loss of I_{Ks}) and LQT2 (HERG-G628S, loss of I_{Kr}) that

☆ All authors take responsibility for all aspects of the reliability and freedom from bias of the data presented and their discussed interpretation.

* Corresponding author at: Heart Center, University of Freiburg, Department of Cardiology and Angiology I, Hugstetter Str. 55, 79106 Freiburg, Germany.
E-mail address: katja.odening@universitaets-herzzentrum.de (K.E. Odening).

https://doi.org/10.1016/j.ijcard.2018.07.050
0167-5273/

mimic the human LQTS disease phenotypes [13] due to pronounced species similarities between rabbits and humans in cardiac ion channels [14], shape of action potential [15], and myocardial tissue velocities [16]. Using TPM-MRI, we have demonstrated regionally heterogeneously impaired diastolic function and prolonged contraction duration in LQT2 rabbits [17], which could predict arrhythmogenic risk better than QTc [18].

Mechanisms leading to mechanical alterations in LQTS and the impact of prolongation of repolarization *per se*, however, remain incompletely understood. To further assemble this puzzle, experiments including molecular, whole organ and *in vivo* levels need to be interpreted together in this highly inter-dependent system of "electro-mechanical feedback".

We hypothesize that the extent of alterations in mechanical myocardial function in LQTS depends on the extent of prolongation of repolarization. Therefore, in the present study, we aimed at gathering further insights into (electro-)mechanical dysfunction and underlying mechanisms in LQT1 (loss of I_{Ks}) and in LQT1 exposed to I_{Kr}-blocker E-4031 (loss of I_{Ks} and reduction of I_{Kr}) compared to WT.

2. Methods

The online supplement contains a more detailed method section.

2.1. Animal studies

Animal experiments were performed in compliance with the German animal protection law (TierSchG), and the Directive 2010/63/EU of the European Parliament after approval by the local authorities (Regierungspraesidium Freiburg; protocol number G11/107).

Male adult transgenic LQT1 ($n = 12$) and wild type (WT, control group, $n = 10$) *New Zealand White* rabbits of similar age and weight were used for *in/ex vivo* experiments (Suppl. Table 1). For molecular analysis, separate age-matched groups of LQT1 and WT rabbits ($n = 4/4$) were added. Rabbits were genotyped by PCR and the phenotype was verified by ECG [13].

S-ketamine (Pfizer, USA) and xylazine (Bayer, Germany) were applied for anesthesia (12.5 mg/kg/3.5 mg/kg IM, followed by IV infusion) during TPM-MRI, ECG transmitter implantation and surface ECG, since this combination does not affect cardiac repolarization [19]. Beating hearts were excised for monophasic action potential recording and molecular analysis after additional injection of heparine (500 IE IV, Braun, Germany) and thiopental-sodium (40 mg/kg IV, Inresa, Germany).

2.2. Surface ECG

Surface ECG were recorded in *sedated* LQT1 and WT rabbits ($n = 12/10$) at baseline and with E-4031 (10 μg/kg bolus and 1 μg/kg/min infusion IV for 20 min) [20].

2.3. Telemetric ECG monitoring

Subcutaneous ECG transmitters were implanted in LQT1 and WT rabbits ($n = 8/7$) as described [13]. QT and RR intervals were determined at baseline and after IM injections of sodium chloride 0.9% (0.33 mL/kg, sham-control) or E-4031 (20 μg/kg, 0.33 mL/kg).

2.4. Tissue phase mapping (TPM-MRI)

To assess regional cardiac function, myocardial longitudinal (Vz) and radial (Vr) tissue velocities were analyzed by TPM-MRI with high spatial and temporal resolution in *sedated* LQT1 and WT rabbits ($n = 12/10$) as described [17]. Systolic and diastolic peak velocities and *time-to* diastolic peak velocities were derived from segmental velocity curves (Fig. 2A/B) acquired at baseline and with E-4031 (10 μg/kg bolus and 1 μg/kg/min infusion IV). Ejection fraction (EF) was calculated based on cine MRI.

2.5. Monophasic action potential duration (APD)

Regional monophasic APD was determined *ex vivo* in the same segments as in TPM-MRI (except for septal segments) at baseline and with E-4031 (0.1 μM) as described [17, 21]. Only hearts without signs of ischemia (as relevant ST segment elevations with APD shortening or visually ischemic tissue) were included (LQT1, $n = 6$; WT, $n = 7$).

2.6. Molecular analysis

Genotype differences in protein and mRNA expression of KvLQT1, HERG, KCNE1, Cav1.2, NCX, PLB, SERCA and RyR were analyzed by Western blot and real-time PCR.

2.7. In silico single cell action potential and tension modeling

Single cell action potentials (AP) were calculated based on the rabbit ventricular cell model by Shannon et al. [22]. In short, the membrane is seen and modulated as a capacitance. Ionic currents are calculated based on their respective gating variables, Nernst potential and the membrane potential. The membrane voltage itself is calculated *via* nonlinear-coupled ordinary differential equations in regard to the ion currents and ion concentrations [23]. To reproduce APs of LQT1, g_{Ks} was set to 0%. The effects of E-4031 were incorporated by decreasing g_{Kr} to 50%.

2.8. Statistical analysis

Statistical analyses were performed with Prism (GraphPad, USA) and Excel (Microsoft, USA). Significance levels of normally distributed data were calculated using *t*-tests. Pearson correlation coefficient was applied for correlation of electrical and mechanical parameters. *p*-Values <0.05 were considered significant.

3. Results

3.1. Electrical (dys-)function

3.1.1. Surface ECG

In surface ECG (Fig. 1A, exemplary ECG traces), QT intervals were longer in *sedated* transgenic LQT1 rabbits compared to WT at baseline (Fig. 1B, baseline: LQT1 226 ± 45 ms *vs.* WT 181 ± 20 ms, $p < 0.01$), while RR intervals were not significantly different (Fig. 1B, baseline: LQT1 415 ± 78 ms *vs.* WT 391 ± 37 ms). This resulted in longer heart-rate corrected QTc (Bazett) in LQT1 than in WT at baseline (LQT1 350 ± 40 ms *vs.* WT 289 ± 24 ms $p < 0.001$). During infusion with I_{Kr}-blocker E-4031, QT intervals became longer in both LQT1 and WT rabbits (Fig. 1B), but QT prolongation (delta) was larger in LQT1 than in WT (Fig. 1C, minute 4: LQT1 + 107 ± 25 ms *vs.* WT +61 ± 21 ms, $p < 0.001$) and similarly, heart-rate corrected QTc was significantly longer in LQT1 (minute 4: LQT1 505 ± 54 ms *vs.* 379 ± 50 ms $p < 0.001$).

3.1.2. ECG telemetry

ECG telemetry in free-moving animals revealed longer baseline QT intervals in LQT1 than in WT (LQT1, 167 ± 13 ms *vs.* WT, 138 ± 12 ms, $p < 0.001$) at similar RR intervals (LQT1 278 ± 25 ms *vs.* WT 256 ± 30 ms). Similarly, heart-rate corrected QTc (Bazett) was longer in LQT1 compared to WT rabbits (LQT1, 317 ± 29 ms *vs.* WT, 274 ± 14 ms, $p < 0.01$). In addition, individual heart-rate corrected QT intervals (QT_{250ms}) were derived from individual QT/RR-regression lines at baseline and after IM injection (Fig. 1D and Suppl. Fig. 1A/B). QT_{250ms} was longer in LQT1 rabbits at baseline (Fig. 1E and Suppl. Fig. 1A), after sham IM injection of NaCl 0.9% (Fig. 1E and Suppl. Fig. 1B), and after injection of E-4031 (Fig. 1D/E) compared to WT. Injection of E-4031 significantly prolonged QT_{250ms} in LQT1 and WT rabbits, while the sham-injection of NaCl 0.9% had no QT_{250ms} prolonging effect (Fig. 1E). Importantly, E-4031-induced prolongation of QT_{250ms} (delta) compared to baseline or NaCl was remarkably larger in LQT1 than in WT rabbits (Suppl. Fig. 1D).

3.1.3. Arrhythmia

No ventricular arrhythmias were detected at baseline or during exposure to E-4031. Due to a pronounced E-4031-induced QT prolongation, pseudo AV-blocks (as described in [24]) developed in two LQT1 during telemetric monitoring (Suppl. Fig. 1E) and in one LQT1 rabbit during MRI, but none developed in WT.

3.1.4. Monophasic action potential duration (APD)

At baseline, APD at 90% of repolarization (APD_{90}) was similar in most regions of LQT1 and WT hearts – except for the apical-anterior segment. During perfusion with E-4031, APD_{90} prolongation was observed in 8 of 11 segments in both, LQT1 and WT hearts (Fig. 1F–H).

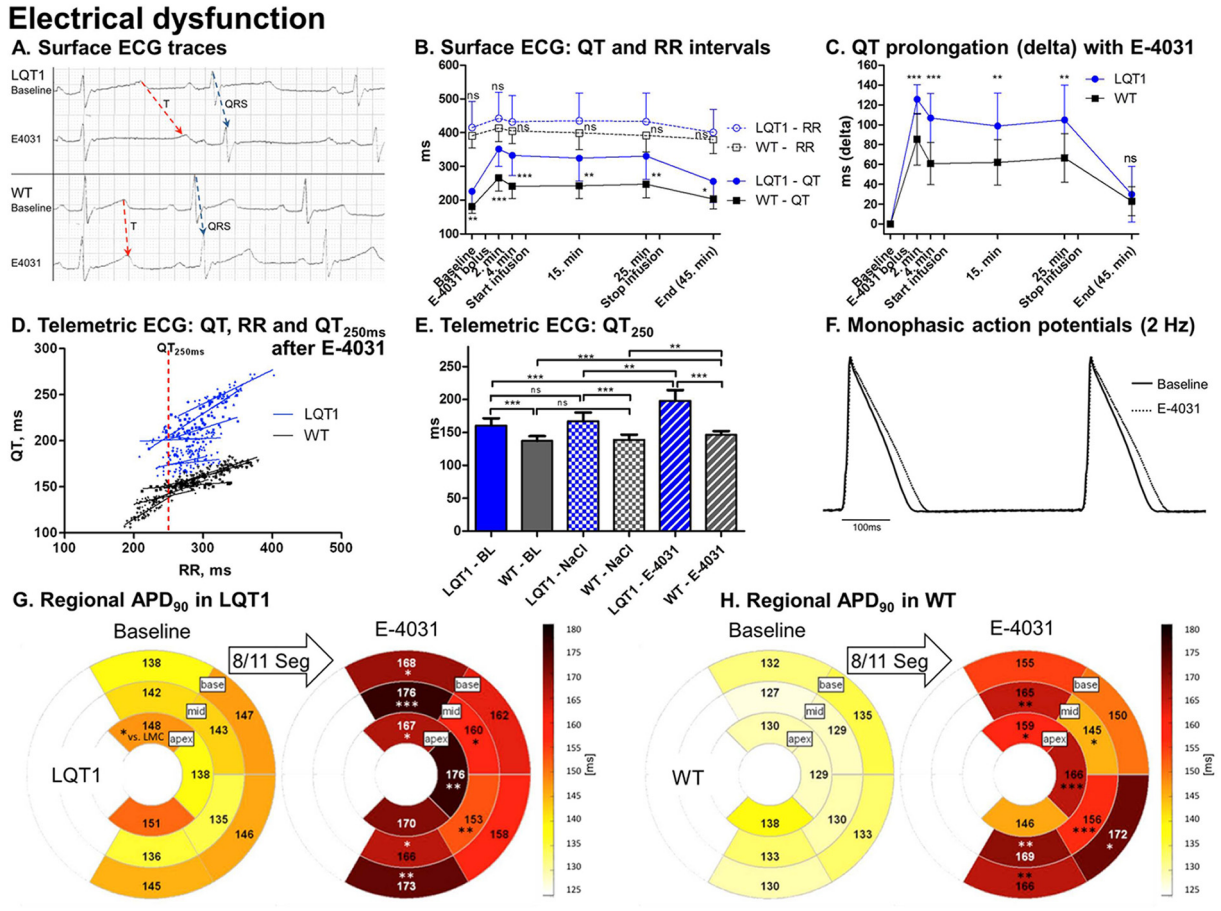

Fig. 1. Electrical dysfunction. Surface ECG (Fig. 1A–C). Protocol: Baseline, bolus of E-4031 (10 μg/kg IV), infusion of E-4031 (1 μg/kg/min IV for 20 min, start to stop). A. Exemplary ECG traces. Larger E-4031-induced QT prolongation (red arrow) in LQT1 and similar RR prolongation (blue arrow). B. Longer QT intervals in LQT1 compared to WT ($n = 12/10$) at baseline and with E-4031, similar RR intervals. C. E-4031 induced a significantly larger QT prolongation (delta) in LQT1. Mean ± SD. Levels of significance using *t*-test: $^{***}p < 0.001$, $^{**}p < 0.01$, $^{*}p < 0.05$, "ns" $p > 0.05$. Telemetric ECG (Fig. 1D/E). D. QT and RR intervals and heart rate corrected QT intervals (QT_{250ms}) after injection of E-4031 (20 μg/kg). E. Longer QT_{250ms} in LQT1 ($n = 8$, blue) compared to WT ($n = 7$, black) at baseline and after injection of NaCl 0.9% or E-4031. Significant prolongation of QT_{250ms} with E-4031 within the groups compared to baseline or injection of NaCl 0.9%. No significant prolongation of QT_{250ms} after NaCl 0,9% compared to baseline. Mean ± SD. Levels of significance using *t*-test: $^{***}p < 0.001$, $^{**}p < 0.01$, $^{*}p < 0.05$, "ns" $p > 0.05$. Monophasic action potentials, stimulation with 2 Hz (Fig. 1F–H). F. Exemplary monophasic action potentials at baseline and with E-4031 (0.1 μM). G/H. Bull's eye-plots, mean regional APD_{90} (4 basal, 4 mid and 3 apical segments) in LQT1 ($n = 6$, G) and WT hearts ($n = 7$, H). E-4031 significantly prolonged APD_{90} in 8/11 segments compared to baseline in LQT1 and WT. Levels of significance using *t*-test: $^{***}p < 0.001$, $^{**}p < 0.01$, $^{*}p < 0.05$, "ns" $p > 0.05$. (For interpretation of the references to color in this figure legend, the reader is referred to the web version of this article.)

3.2. Mechanical (dys-)function

3.2.1. Systolic function

Ejection fraction (EF) – a marker for global systolic function – was similar in both groups at baseline and was preserved upon E-4031 infusion (Suppl. Table 2).

At baseline, LQT1 and WT rabbits had similar regional longitudinal (Vz, Fig. 2C) and radial systolic peak velocities (Vr, Suppl. Fig. 2A). E-4031, however, increased systolic peak velocities in 16 (Vz) and 10 (Vr) of 16 LV segments in LQT1 hearts (Fig. 2C and Suppl. Fig. 2A), indicating improved systolic function. Of note, enhancement of systolic function was particularly pronounced in LV base and mid (Fig. 2D). In WT, in contrast, systolic peak velocities were increased only in 1 of 16 segments in Vr and were unchanged in Vz (Fig. 2C and Suppl. Fig. 2A). The E-4031-induced increase (delta) of systolic peak Vz and Vr was larger in LQT1 than in WT in almost all segments, reaching statistical significance in 7 segments in the longitudinal (Fig. 2D) and 5 segments in the radial direction (Suppl. Fig. 2B).

3.2.2. Diastolic function

At baseline, diastolic peak Vz were similar in LQT1 and WT hearts (Vz, Fig. 2E), and diastolic peak Vr differed in only two LV segments (apex-anterior und apex-septal, Vr, Suppl. Fig. 2C). E-4031 reduced diastolic peak velocities in LQT1 rabbits in 12 (Vz) and 9 (Vr) of 16 segments (Fig. 2E and Suppl. Fig. 2C), indicating E-4031-induced diastolic dysfunction. In WT, in contrast, E-4031 decreased diastolic peak Vz only in 3 of 16 LV segments (Fig. 2E), while diastolic peak Vr remained unchanged (Suppl. Fig. 2C). E-4031-induced decrease in diastolic peak velocities (delta) was significantly larger in LQT1 in 9 segments in the longitudinal (Fig. 2F) and 5 segments in the radial (Suppl. Fig. 2D) direction compared to WT rabbits.

Time-to diastolic peak Vz and Vr – a marker for contraction duration – was similar in both groups at baseline, and only minor alterations were found with E-4031 (Suppl. Fig. 2E/F).

3.3. Electro-mechanical correlation

To investigate a potential correlation between electrical and mechanical function, pooled (WT and LQT1) electrical (QT interval) and mechanical data (peak diastolic velocities, averaged basal and mid segments) were analyzed. After infusion of E-4031 (Fig. 3A), QT duration correlated significantly with (lower) radial and longitudinal diastolic peak velocities (Vz: $r = -0.59$, $p < 0.01$, Vr: $r = -0.48$, $p < 0.05$; Fig. 3A). Moreover, the extent of E-4031-induced QT prolongation (delta-QT) correlated with the extent of E-4031-induced decrease

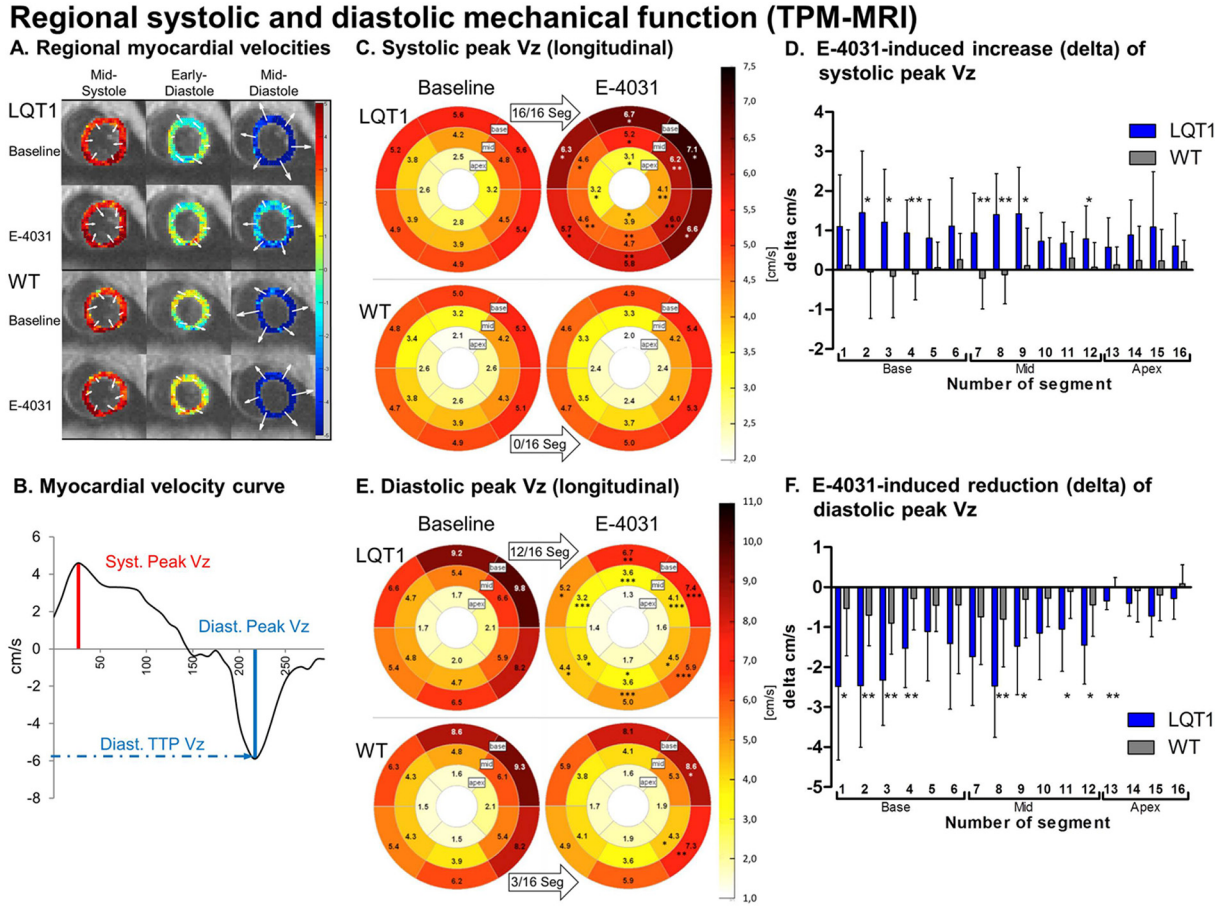

Fig. 2. Regional systolic and diastolic mechanical function (TPM-MRI). A. Exemplary regional longitudinal (Vz, color-coded) and radial (Vr, length of white arrows) myocardial velocities in LQT1 and WT rabbits (basal segments): lighter blue in LQT1 indicates decreased diastolic peak Vz. B. Myocardial velocity curve (averaged LQT1 basal segments at baseline, $n = 12$) indicating systolic and diastolic peak Vz and time-to diastolic peak Vz (TTP). C + E. Bull's eye-plots (6 basal, 6 mid and 4 apical segments) of LQT1 and WT ($n = 12/10$) rabbits displaying mean systolic (C) and diastolic (E) peak Vz. Similar peak longitudinal velocities at baseline in LQT1 and WT rabbits. Only in LQT1 rabbits, E-4031 significantly increased systolic peak Vz (C). E-4031 decreased diastolic peak Vz in LQT1 in 12 segments, but only in 3 segments in WT rabbits (E). D + F. E-4031-induced change (delta) of systolic/diastolic peak Vz in the different segments: the increase of systolic peak VZ was more pronounced in LQT1 than in WT in 7 segments (D). The decrease of diastolic peak Vz was more pronounced in LQT1 in 9 segments (F). Levels of significance using *t*-test: $^{***}p < 0.001$, $^{**}p < 0.01$, $^{*}p < 0.05$. (For interpretation of the references to color in this figure legend, the reader is referred to the web version of this article.)

of diastolic peak velocities (delta-diastolic velocity) (Vz, $r = -0.617$, $p < 0.01$; Vr, $r = -0.621$, $p < 0.01$; Fig. 3B).

Correlation of electrical and mechanical parameters within the separate groups (LQT1 or WT) did not reach significance due to small group size and outliers. Additionally, in contrast to previous studies in LQT2 [17] regional diastolic peak velocities did not correlate with regional APD_{90} to a relevant extent (significance reached only in one segment in LQT1 with E-4031), likely due to the less pronounced mechanical alterations in LQT1 compared to LQT2.

3.4. In silico single cell action potential and tension modeling

To investigate whether a sole reduction of I_{Ks} and/or I_{Kr} (and resulting prolongation of repolarization) may result in the observed changes in mechanical function, we performed *in silico* single cell modeling. Similarly as observed experimentally, loss of I_{Ks} (0% g_{Ks}, LQT1 at baseline) resulted in a slight APD prolongation (Fig. 3C) and the reduction of g_{Kr} had a similarly pronounced APD-prolonging effect as E-4031 in the experimental setting (Fig. 3C).

Peak velocity in tension development and relaxation (Fig. 3D, slope steepness of upstroke and downstroke) were used as estimate for measured peak systolic and diastolic velocities. Similarly as observed, 50% reduction of g_{Kr} (E-4031) increased velocity of tension development and decreased relaxation velocity – particularly in absence of g_{Ks} (LQT1 + E-4031).

3.5. Differences in ion channel and Ca^{2+} handling protein expression

In transgenic LQT1 rabbits that are over-expressing the human *loss-of-function*-mutated KvLQT1/KCNQ1 [13], expression of total KvLQT1/KCNQ1 (endogenous + transgenic mutated channels) was increased compared to WT hearts (only expressing endogenous KvLQT1/KCNQ1; Fig. 4A). The beta-subunit KCNE1, in contrast, was down regulated in LQT1 compared to WT (Fig. 4B), both contributing to lower/absent I_{Ks} current in LQT1 cardiomyocytes [13]. Kir2.1/I_{K1} and Cav1.2/$I_{Ca,L}$ were similarly expressed in both groups (Suppl. Fig.3). SERCA protein and mRNA levels were not altered. Small changes were observed in other Ca^{2+} handling proteins: Phospholamban (PLB) was decreased in LQT1 (Fig. 4C) and RyR tended to be reduced in LQT1 hearts (Fig. 4D). On the mRNA level, *NCX* was increased in LQT1 hearts (Fig. 4E).

4. Discussion

4.1. Electrical (dys-)function in LQT1 rabbits

Due to the over-expression of *loss-of-function* mutated KvLQT1/I_{Ks} (KvLQT1-Y315S), *in vivo* QT intervals were longer in transgenic LQT1 than in WT rabbits in the present and previous studies [13]. E-4031 induced a larger QT prolongation in *sedated* and *free-moving* LQT1 compared to WT rabbits. Monophasic APD, in contrast, measured *ex vivo* –

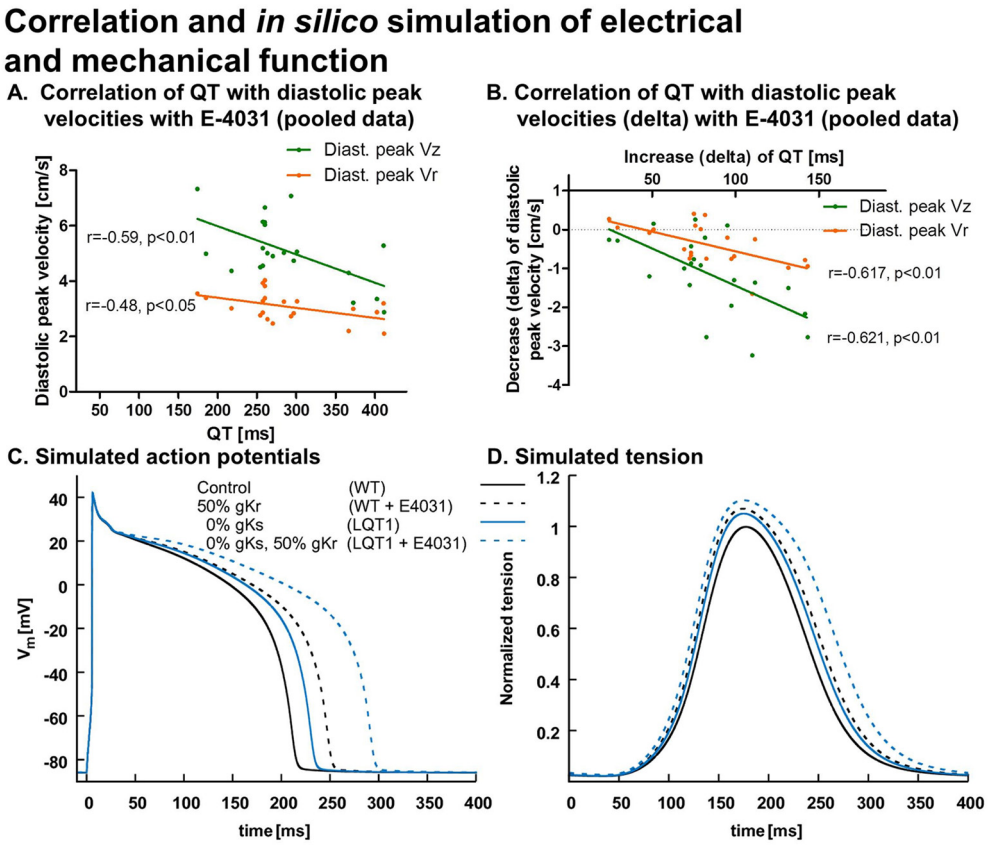

Fig. 3. Correlation and *in silico* simulation of electrical and mechanical function. A/B. Electro-mechanical correlation in pooled LQT1 and WT rabbits ($n = 21$). Significant correlation (Pearson correlation coefficient, r) of the QT interval (A) and the increase of the QT interval (delta, B) with decreased longitudinal (Vz) and radial (Vr) diastolic peak velocities with E-4031. C/D. *In silico* simulation of action potential and tension. A. Simulation of action potentials (AP) with longer AP in LQT1 (loss of I_{Ks}, 0% g_{Ks}) compared to control (WT). Additional reduction of g_{Kr} (50% g_{Kr}) pronouncedly prolonged the AP (as E-4031). B. Simulation of tension development. Reduction of g_{Kr} (E-4031, 50% g_{Kr}) increased the steepness of the slope upstroke and decreased the steepness of the slope downstroke as compared to LQT1.

hence without physiological autonomic influence – were not significantly longer in LQT1 hearts at baseline as reported previously [21].

4.2. Mechanical (dys-)function in LQT1 rabbits

Global mechanical function (ejection fraction) was similar in LQT1 and WT rabbits, as previously observed with conventional imaging in LQTS patients [6, 8, 9] and rabbits [13]. In contrast, subtle abnormalities of myocardial systolic and diastolic function in LQTS, such as alterations in contraction pattern [4], contraction duration or its dispersion have been identified in LQTS and were associated with higher occurrence of arrhythmia [4, 6–8, 10].

In our study, we used TPM-MRI to analyze regional changes in mechanical function secondary to LQTS-related electrical alterations. Regional systolic and diastolic peak velocities were unaltered in LQT1 hearts at baseline, while we have previously identified impaired diastolic function in LQT2 rabbits [17]. This observation may be partially attributed to a minor contribution of I_{Ks} to repolarization compared to I_{Kr} in the rabbit [25] and a less pronounced QT/APD prolongation in LQT1 compared to LQT2 [13]. In line with this observation, diastolic function was particularly impaired in LQT2 rabbit hearts with very pronounced APD prolongation as compared to those with less pronounced APD prolongation [13]. Although mechanical function was altered in LQT1 patients [6–9], in human LQT1, myocardial mechanical function (longitudinal strain) was less pronouncedly impaired than in human LQT2 [8] – similarly as observed in the transgenic rabbit models.

Upon I_{Kr}-blockade, in contrast, pronounced differences were unmasked between LQT1 and WT hearts. The E-4031-induced QT prolongation in LQT1 matched with an E-4031-induced decrease of regional diastolic peak velocities in LQT1. Importantly, in pooled analysis of basal and mid segments, the extent of diastolic mechanical impairment significantly correlated with QT duration and prolongation after administration of E-4031, indicating that the mechanical diastolic impairment in LQTS depends on the (extent of) primary electrical alterations.

While E-4031/I_{Kr}-blockade has previously been shown to increase contractility and impair diastolic relaxation in healthy mammalian hearts of various species [26], we here demonstrate that E-4031 induces a particularly pronounced (regionally heterogeneous) amelioration of systolic function and reduction of diastolic relaxation only in LQT1. Of note, this is in contrast with the observation of normal (to slightly decreased) systolic function in LQT2 rabbits and patients [6–8, 13].

These observations indicate that both the extent of impairment of global repolarization as well as the impairment of a defined repolarizing ion current (I_{Ks} or I_{Kr}) may affect the extent of alterations in mechanical function in LQT1 (loss of I_{Ks}) and LQT2 rabbits (loss of I_{Kr}). As genotype differences in the extent of mechanical impairment are present in both, rabbit and human LQTS subjects, these experimental models provide important insights into the importance of the reduction of a defined repolarizing current (I_{Ks} or I_{Kr}) and the extent of the prolongation of repolarization for LQTS-related mechanical impairment. To precisely identify the relative importance of dose-dependent electrical alterations for mechanical alterations and the differential quantitative contribution of reduced I_{Kr} and/or I_{Ks} to mechanical alterations, however, future experiments exposing LQT1, LQT2, and WT rabbits to different dosages of I_{Kr} and/or I_{Ks} blockers are warranted.

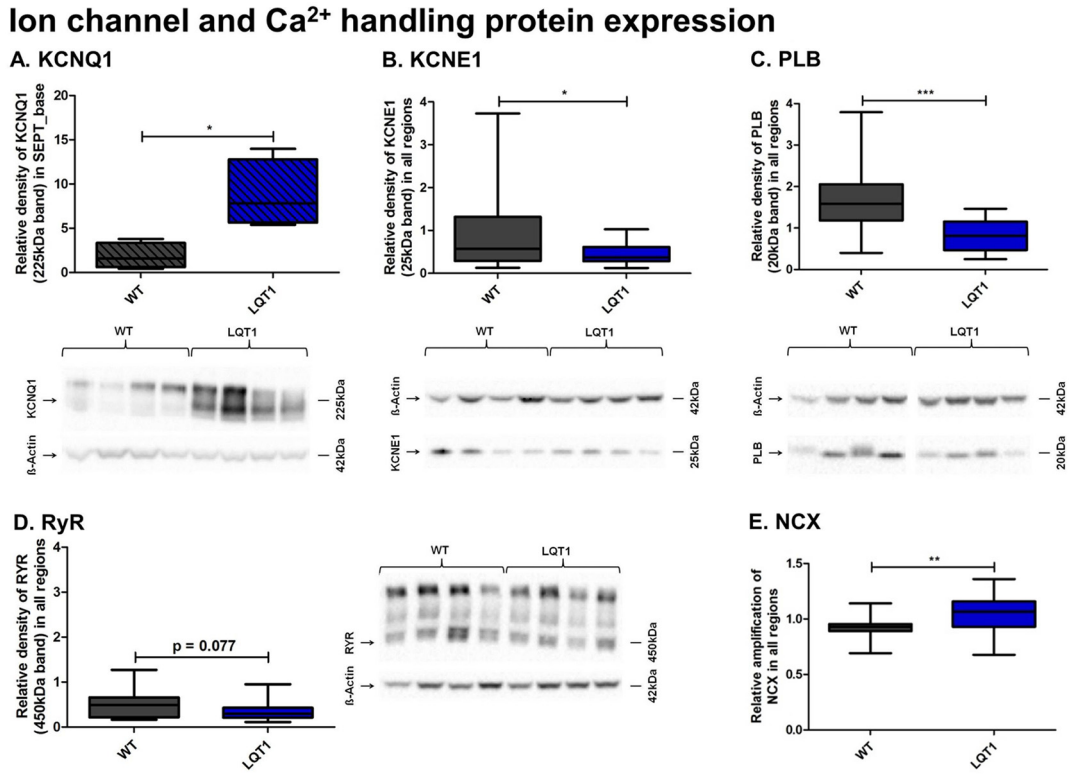

Fig. 4. Ion channel and Ca^{2+} handling protein expression. A–D. Box plots indicating relative protein expression in LQT1 and WT hearts ($n = 4/4$) with representative Western blot (WB) below/to the right. Beta-Actin expression was used as loading control. A. KCNQ1 expression in Septum base. WB of KCNQ1 in Septum base. B. KCNE1 expression in all regions. WB of KCNE1 in LV apex. C. PLB expression in all regions. WB of PLB in Septum mid. D. RyR expression in LV base. WB of RyR in LV base. E. Box plot indicating relative mRNA amplification of *NCX* in all regions. Levels of significance using *t*-test: $^{***}p < 0.001$, $^{**}p < 0.01$, $^{*}p < 0.05$.

4.3. Mechanisms underlying genotype differences in electro-mechanical function

In LQT1 hearts, we observed a greater expression of KvLQT1/KCNQ1 channels (mutated human and endogenous rabbit subunits) compared to WT as described [13]. KCNE1 was reduced in LQT1 hearts, also contributing to reduced/absent I_{Ks} in LQT1 cardiomyocytes, but expression of the remaining repolarizing current Kir2.1/I_{K1} was unaltered. The resulting reduced repolarization reserve may explain the increased susceptibility to E-4031-induced QT prolongation and alterations of (regional) mechanical function particularly in LQT1 hearts. Due to electro-mechanical coupling, we suggest that I_{Kr}-blocker-induced prolongation of repolarization further prolongs Ca^{2+}-influx *via* $I_{Ca,L}$, increases intracellular calcium concentration, and prolongs Ca^{2+} transients, causing an increase in contractility/increased systolic peak velocities [27, 28], and impaired relaxation/reduced diastolic peak velocities [26]. In this line, De Ferrari et al. [29] observed that calcium channel blockers eliminated abnormal contraction patterns in LQTS [4], suggesting a causative role of intracellular calcium for LQTS-associated mechanical dysfunction [5, 29].

In silico cellular tension models confirmed the experimental observation of increased steepness of slope upstroke (increased systolic peak velocity) and decreased steepness of slope downstroke (decreased diastolic peak velocity) upon reduction of g_{Kr} (E-4031) – particularly in the setting of absent g_{Ks} (LQT1) – thus highlighting that further prolongation of repolarization by I_{Kr}-blockade may unmask subtle mechanical impairment in LQT1.

In addition to the alterations in repolarization, the small changes in Ca^{2+} handling proteins might also (partly) contribute to altered mechanics in LQT1. As NCX affects systolic mechanical function *via* its reverse mode activity [30], NCX over-expression improved systolic function in a rabbit heart-failure model, while it had no mechanical effects in normal hearts [31]. Similarly, the increased NCX transcription in LQT1 hearts might not be sufficient to change mechanical function at baseline but may contribute to improved systolic function (increased systolic peak velocities) if the system is further stressed by E-4031. Here the assessment of functional changes in NCX activity and resulting calcium transient characteristics are warranted in the future; particularly as the impact of NCX on mechanical function is already rather complex in the physiological setting and might be further modified in the setting of prolonged APD.

Experimental data further suggest that a reduction of PLB as observed in LQT1 hearts and consecutive reduced inhibition of SERCA function [32] might similarly improve systolic function as in a mouse heart failure model, in which a knock-out of PLB rescued systolic function [33]. As SERCA expression, however, was unaltered in LQT1 hearts, its relevance needs to be evaluated in functional assays.

4.4. Limitations

Baseline mechanical function in LQT1 rabbit hearts was not impaired, although one might expect some mechanical dysfunction based on observations in human patients. This may be partially attributed to a minor contribution of I_{Ks} to repolarization compared to I_{Kr} in the rabbit at baseline conditions [25]. Furthermore, as LQT1 associated symptoms and QT prolongation are particularly associated with sympathetic stimulation [1, 13, 34, 35], mechanical consequences of LQT1 might be more apparent when assessed with intact autonomic influence.

In the present study, data on electrical (APD *ex vivo*, ECG *in vivo*) and mechanical cardiac function (TPM-MRI) were acquired sequentially in each LQT1 and WT rabbit. Protocols for anesthesia and E-4031 infusion were equal during surface ECG and TPM-MRI, thus qualifying for correlation. However, an ideal experimental setup for electro-mechanical

assessment (and correlation) would allow simultaneous recording of regional electrical and mechanical data *in vivo*. In the future, MR-compatible EP catheters might help to overcome these technical limitations.

To identify mechanisms accounting for altered electro-mechanical function in LQT1, we assessed regional transcription and protein expression of ion channels and Ca^{2+} handling proteins. To fully understand the impact of altered ion channels/Ca^{2+} handling proteins for electro-mechanical alterations in LQTS, analyses of their phosphorylation state and functional changes in their activity and resulting calcium transient characteristics are warranted in the future; particularly as the impact of several Ca^{2+} handling proteins is already rather complex in the physiological setting and might be further modified in the setting of prolonged APD.

4.5. Clinical/translational implications

In line with experimental and clinical studies [4–12, 17, 18, 29] this study confirms that LQTS constitutes an electro-mechanical disorder. Studies in LQTS patients [4, 6–8, 10] and LQT2 rabbits [18] could previously link mechanical dysfunction with an increased arrhythmic risk. With the present study we demonstrate that the extent of QT prolongation correlates with impairment of diastolic function upon administration of E-4031. Furthermore, we identify genotype differences in the extent of mechanical impairment in LQTS: In contrast to LQT2 rabbits (with pronounced QT prolongation and mechanical dysfunction) [17], LQT1 rabbits (with moderate QT prolongation) lack baseline mechanical impairment, but show amelioration of systolic and impairment of diastolic function upon further prolongation of repolarization. Of note, this phenomenon could be of clinical importance in undiagnosed or subclinical LQTS with concomitant administration of QT-prolonging drugs [2].

These data indicate an importance of the *extent* of QT prolongation and of the contribution of different impaired repolarizing current for conveying mechanical dysfunction. Increasing our understanding of genotype differences in electro-mechanical dysfunction might allow future genotype-specific risk assessment using a combined assessment of electrical and mechanical parameters.

4.6. Conclusions

While baseline mechanical function was normal in LQT1 rabbits despite a distinct QT prolongation, further prolongation of repolarization by I_{Kr}-blocker E-4031 unmasked mechanical alterations with amelioration of systolic function and impairment of diastolic relaxation LQT1. These data indicate an importance of the *extent* of QT prolongation and the contribution of different impaired ion currents for conveying mechanical dysfunction.

Funding sources

This research was supported by the “Margarete von Wrangell Habilitation Program” by the Ministry of Sciences, Research, and Arts in Baden Wuerttemberg and the European Social Fund to Dr. K.E. Odening.

Disclosures/COI

The authors report no relationships that could be construed as a conflict of interest.

Appendix A. Supplementary data

Supplementary data to this article can be found online at https://doi.org/10.1016/j.ijcard.2018.07.050.

References

[1] P.J. Schwartz, L. Crotti, R. Insolia, Long-QT syndrome: from genetics to management, Circ. Arrhythm. Electrophysiol. 5 (2012) 868–877.
[2] D.M. Roden, Drug-induced prolongation of the QT interval, N. Engl. J. Med. 350 (2004) 1013–1022.
[3] C. Antzelevitch, Role of spatial dispersion of repolarization in inherited and acquired sudden cardiac death syndromes, Am. J. Physiol. Heart Circ. Physiol. 293 (2007) H2024–H2038.
[4] F. Nador, G. Beria, G.M. de Ferrari, et al., Unsuspected echocardiographic abnormality in the long QT syndrome. Diagnostic, prognostic, and pathogenetic implications, Circulation 84 (1991) 1530–1542.
[5] G.M. de Ferrari, P.J. Schwartz, Vox clamantis in deserto. We spoke but nobody was listening: echocardiography can help risk stratification of the long-QT syndrome, Eur. Heart J. 36 (2015) 148–150.
[6] K.H. Haugaa, T. Edvardsen, T.P. Leren, J.M. Gran, O.A. Smiseth, J.P. Amlie, Left ventricular mechanical dispersion by tissue Doppler imaging: a novel approach for identifying high-risk individuals with long QT syndrome, Eur. Heart J. 30 (2009) 330–337.
[7] K.H. Haugaa, J.P. Amlie, K.E. Berge, T.P. Leren, O.A. Smiseth, T. Edvardsen, Transmural differences in myocardial contraction in long-QT syndrome: mechanical consequences of ion channel dysfunction, Circulation 122 (2010) 1355–1363.
[8] I.S. Leren, N.E. Hasselberg, J. Saberniak, et al., Cardiac mechanical alterations and genotype specific differences in subjects with long QT syndrome, JACC Cardiovasc. Imaging 8 (2015) 501–510.
[9] J. Brado, M.J. Dechant, M. Menza, et al., Phase-contrast magnet resonance imaging reveals regional, transmural, and base-to-apex dispersion of mechanical dysfunction in patients with long QT syndrome, Heart Rhythm. 14 (2017) 1388–1397.
[10] R.M.A. ter Bekke, K.H. Haugaa, A. van den Wijngaard, et al., Electromechanical window negativity in genotyped long-QT syndrome patients: relation to arrhythmia risk, Eur. Heart J. 36 (2015) 179–186.
[11] C. Savoye, D. Klug, I. Denjoy, et al., Tissue Doppler echocardiography in patients with long QT syndrome, Eur. J. Echocardiogr. 4 (2003) 209–213.
[12] G.M. de Ferrari, P.J. Schwartz, Long QT syndrome, a purely electrical disease? Not anymore, Eur. Heart J. 30 (2009) 253–255.
[13] M. Brunner, X. Peng, G.X. Liu, et al., Mechanisms of cardiac arrhythmias and sudden death in transgenic rabbits with long QT syndrome, J. Clin. Invest. 118 (2008) 2246–2259.
[14] J.M. Nerbonne, Molecular basis of functional voltage-gated K+ channel diversity in the mammalian myocardium, J. Physiol. 525 (Pt 2) (2000) 285–298.
[15] A. Varro, D.A. Lathrop, S.B. Hester, P.P. Nanasi, J.G. Papp, Ionic currents and action potentials in rabbit, rat, and guinea pig ventricular myocytes, Basic Res. Cardiol. 88 (1993) 93–102.
[16] B. Jung, K.E. Odening, E. Dall'Armellina, et al., A quantitative comparison of regional myocardial motion in mice, rabbits and humans using in-vivo phase contrast CMR, J. Cardiovasc. Magn. Reson. 14 (2012) 87.
[17] K.E. Odening, B.A. Jung, C.N. Lang, et al., Spatial correlation of action potential duration and diastolic dysfunction in transgenic and drug-induced LQT2 rabbits, Heart Rhythm. 10 (2013) 1533–1541.
[18] C.N. Lang, M. Menza, S. Jochem, et al., Electro-mechanical dysfunction in long QT syndrome: role for arrhythmogenic risk prediction and modulation by sex and sex hormones, Prog. Biophys. Mol. Biol. 120 (2016) 255–269.
[19] K.E. Odening, O. Hyder, L. Chaves, et al., Pharmacogenomics of anesthetic drugs in transgenic LQT1 and LQT2 rabbits reveal genotype-specific differential effects on cardiac repolarization, Am. J. Physiol. Heart Circ. Physiol. 295 (2008) H2264–H2272.
[20] G. Michael, J. Dempster, K.A. Kane, S.J. Coker, Potentiation of E-4031-induced torsade de pointes by HMR1556 or ATX-II is not predicted by action potential short-term variability or triangulation, Br. J. Pharmacol. 152 (2007) 1215–1227.
[21] D. Ziupa, J. Beck, G. Franke, et al., Pronounced effects of HERG-blockers E-4031 and erythromycin on APD, spatial APD dispersion and triangulation in transgenic long-QT type 1 rabbits, PLoS One 9 (2014), e107210. .
[22] T.R. Shannon, F. Wang, J. Puglisi, C. Weber, D.M. Bers, A mathematical treatment of integrated Ca dynamics within the ventricular myocyte, Biophys. J. 87 (2004) 3351–3371.
[23] M. Fink, S.A. Niederer, E.M. Cherry, et al., Cardiac cell modelling: observations from the heart of the cardiac physiome project, Prog. Biophys. Mol. Biol. 104 (2011) 2–21.
[24] M.B. Rosenbaum, R.S. Acunzo, Pseudo 2:1 atrioventricular block and T wave alternans in the long QT syndromes: 1 atrioventricular block and T wave alternans in the long QT syndromes, J. Am. Coll. Cardiol. 18 (1991) 1363–1366.
[25] C. Lengyel, N. Iost, L. Virag, A. Varro, D.A. Lathrop, J.G. Papp, Pharmacological block of the slow component of the outward delayed rectifier current (I(Ks)) fails to lengthen rabbit ventricular muscle QT(c) and action potential duration, Br. J. Pharmacol. 132 (2001) 101–110.
[26] H.E. Cingolani, R.T. Wiedmann, J.J. Lynch, et al., Negative lusitropic effect of DPI 201-106 and E4031. Possible role of prolonging action potential duration, J. Mol. Cell. Cardiol. 22 (1990) 1025–1034.
[27] P.H. Backx, W.D. Gao, M.D. Azan-Backx, E. Marban, The relationship between contractile force and intracellular Ca^{2+} in intact rat cardiac trabeculae, J. Gen. Physiol. 105 (1995) 1–19.
[28] R.A. Bassani, Transient outward potassium current and Ca^{2+} homeostasis in the heart: beyond the action potential, Braz. J. Med. Biol. Res. 39 (2006) 393–403.
[29] G.M. de Ferrari, F. Nador, G. Beria, S. Sala, A. Lotto, P.J. Schwartz, Effect of calcium channel block on the wall motion abnormality of the idiopathic long QT syndrome, Circulation 89 (1994) 2126–2132.
[30] M. Lorenz, N. Hellige, P. Rieder, et al., Positive inotropic effects of epigallocatechin-3-gallate (EGCG) involve activation of Na^+/H^+ and Na^+/Ca^{2+} exchangers, Eur. J. Heart Fail. 10 (2008) 439–445.

[31] G. Munch, K. Rosport, C. Baumgartner, et al., Functional alterations after cardiac sodium-calcium exchanger overexpression in heart failure, Am. J. Physiol. Heart Circ. Physiol. 291 (2006) H488–H495.
[32] N.-A.D. Ablorh, D.D. Thomas, Phospholamban phosphorylation, mutation, and structural dynamics: a biophysical approach to understanding and treating cardiomyopathy: a biophysical approach to understanding and treating cardiomyopathy, Biophys. Rev. 7 (2015) 63–76.
[33] S. Rajan, J.R. Pena, A.G. Jegga, B.J. Aronow, B.M. Wolska, D.F. Wieczorek, Microarray analysis of active cardiac remodeling genes in a familial hypertrophic cardiomyopathy mouse model rescued by a phospholamban knockout, Physiol. Genomics 45 (2013) 764–773.
[34] W. Shimizu, T. Kurita, K. Matsuo, et al., Improvement of repolarization abnormalities by a K^+ channel opener in the LQT1 form of congenital long-QT syndrome, Circulation 97 (1998) 1581–1588.
[35] K.E. Odening, M. Kirk, M. Brunner, et al., Electrophysiological studies of transgenic long QT type 1 and type 2 rabbits reveal genotype-specific differences in ventricular refractoriness and his conduction, Am. J. Physiol. Heart Circ. Physiol. 299 (2010) H643–H655.